



ELSEVIER

Contents lists available at [ScienceDirect](https://www.sciencedirect.com)

## Journal of Hydrology: Regional Studies

journal homepage: [www.elsevier.com/locate/ejrh](http://www.elsevier.com/locate/ejrh)

# Hazards of sea level rise and dams built on the River Nile on water budget and salinity of the Nile Delta aquifer

Ismail Abd-Elaty<sup>a,\*</sup>, Alban Kuriqi<sup>b,c</sup>, Elsayed M. Ramadan<sup>a</sup>, Ashraf A. Ahmed<sup>d,\*</sup>

<sup>a</sup> Department of Water and Water Structures Engineering, Faculty of Engineering, Zagazig University, Zagazig 44519, Egypt

<sup>b</sup> CERIS, Instituto Superior Técnico, Universidade de Lisboa, Av. Rovisco Pais 1, 1049-001 Lisbon, Portugal

<sup>c</sup> Civil Engineering Department, University for Business and Technology, Pristina, Kosovo

<sup>d</sup> Department of Civil and Environmental Engineering, Brunel University London, Uxbridge UB83PH, UK

## ARTICLE INFO

## Keywords:

Grand Ethiopian Renaissance Dam

Hydropower

Water abstraction

Water budget

Water crisis

Seawater Intrusion

Nile Delta Aquifer

## ABSTRACT

**Study region:** The Nile Delta region consists of flat, low-lying areas, where most areas are used for agriculture. It covers an area of 22,000 km<sup>2</sup>, which is 2.20% of the total area of Egypt.

**Study focus:** This study evaluates the water budget and the salinity due to the Sea Level Rise (SLR) and the reduction in the river water flow caused by the Grand Ethiopian Renaissance Dam (GERD) using the numerical code SEAWAT. Three filling scenarios were considered for the GERD reservoir at elevations 600 m, 621 m, and 645 m above mean sea level (AMSL) for the storage volumes of 17 billion cubic meters (BCM) (scenarios #1), 37.30 BCM (scenarios #2), and 74 BCM (scenarios #3). The impact of these fillings scenarios was combined with SLR of 25 cm, and increasing the abstraction rates from the Nile Delta aquifer by 25%, 50%, and 100%, respectively.

**New hydrological insights for the region:** The study findings indicated that the SLR and the GERD reservoir filling with increasing pumping rates, especially during the filling periods, would influence the groundwater resources in the Nile Delta. The GERD reservoir filling could alter the freshwater, in which the aquifer salinity increased by 4.47%, 11.48%, and 29.99% for the three scenarios, respectively. The methodology and findings presented in this study might be useful for investing and comparing the impact of SLR and upstream dam projects on the downstream water budget and salinity at other coastal regions.

## 1. Introduction

Global warming due to climate change seriously affects the hydrologic cycle components by changing their quantity and quality in space, time, and frequency domains (Abd-Elaty et al., 2021; Sherif and Singh, 1999). Coastal areas are considerably affected in the long term because of climate change and anthropogenic factors (Harley et al., 2006). The consequences include Sea Level Rise (SLR), subsidence of shore cities, increased coastal erosion, and seawater intrusion (Canning, 2001; El Shinawi et al., 2022b; Abd-Elaty et al., 2022a).

Based on the intergovernmental panel on climate change, the global mean SLR reached 1–2 mm.yr<sup>-1</sup> by the end of the last century (Cai et al., 2022). Long-term climate projections indicate a global mean SLR of 0.30 – 0.65 m (Kumar, 2012). Oude Essink and Schaars (2003) investigated the quantitative and qualitative effects on groundwater due to climate change, SLR, land subsidence, and human

\* Corresponding authors.

E-mail addresses: [Eng\\_abdelaty2006@yahoo.com](mailto:Eng_abdelaty2006@yahoo.com), [Eng\\_abdelaty@zu.edu.eg](mailto:Eng_abdelaty@zu.edu.eg) (I. Abd-Elaty), [Ashraf.ahmed@brunel.ac.uk](mailto:Ashraf.ahmed@brunel.ac.uk) (A.A. Ahmed).

<https://doi.org/10.1016/j.ejrh.2023.101600>

Received 31 December 2022; Received in revised form 1 December 2023; Accepted 3 December 2023

Available online 15 December 2023

2214-5818/© 2023 The Authors. Published by Elsevier B.V. This is an open access article under the CC BY license (<http://creativecommons.org/licenses/by/4.0/>).

activities. Tiruneh and Motz (2003) studied the effect of SLR on freshwater alteration due to saltwater intrusion (SWI) under different scenarios. The changes in sea levels and the global mean surface temperature can also affect precipitation quantities, timings, and intensity. Moreover, other associated impacts may include saltwater intrusion (SWI) and water shortage.

Excessive pumping due to increasing water demands along coastal areas has dramatically caused SWI problems. Bear (2012) proposed optimizing model for SWI based on the abstraction rates. Aharmouch et al. (2001) and Guo and Langevin (2002) predicted the position of SWI of sharp interface in coastal aquifers resulting from extensive groundwater exploitation. Narayan et al. (2002) investigated the presence of the SWI in the Burdekin Delta aquifer under different recharge conditions and pumping scenarios using the SUTRA model. Qahman and Larabi (2006) employed and studied the massive SWI in Gaza’s aquifer, Palestinian, using different abstraction rates with transit state. Mabrouk et al. (2019) simulated the SLR and groundwater pumping combination on the Nile Delta Aquifer (NDA) using the SEAWAT code. Results of the study showed that the SWI is a long-term process and will cause future losses in

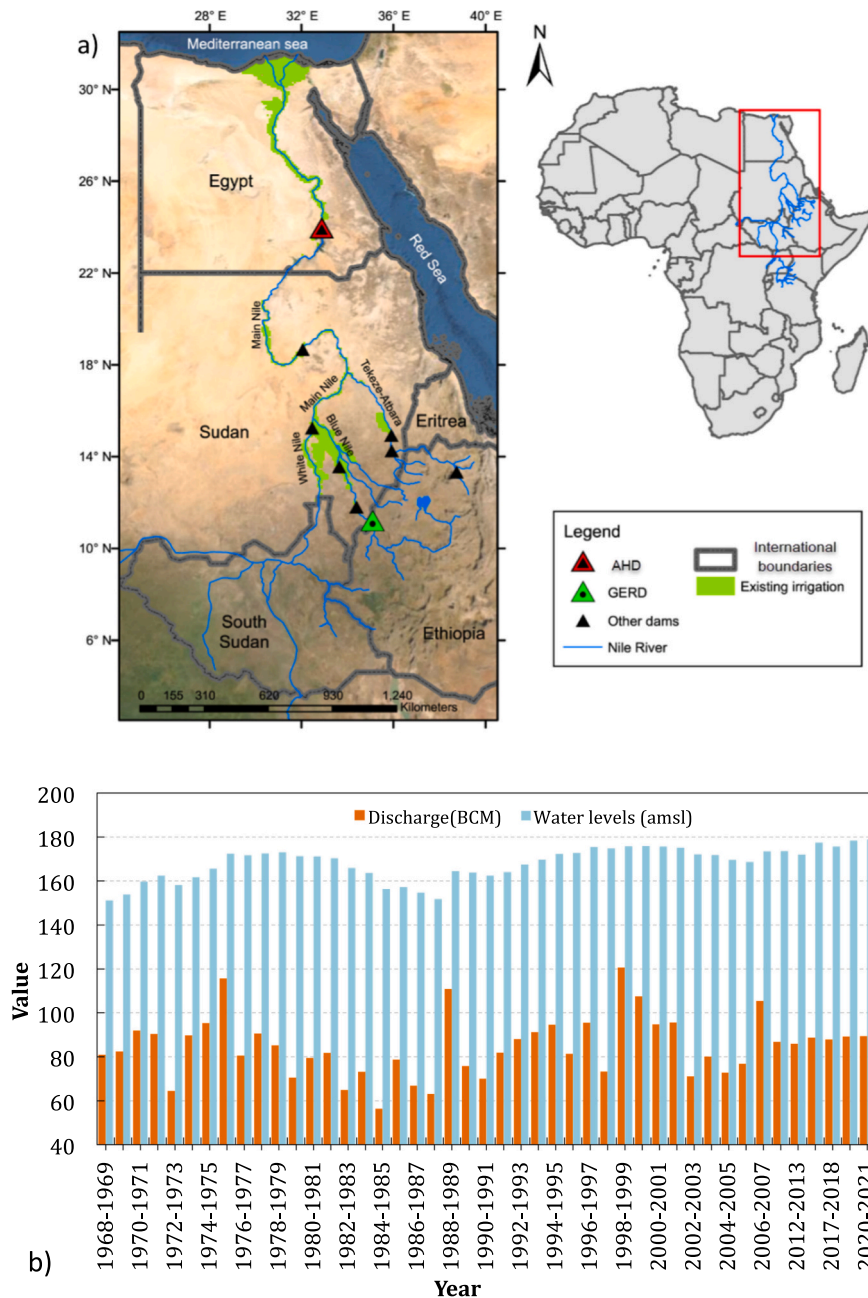


Fig. 1. River Nile basin: a) Location of the GERD within the Nile River catchment area, after Basheer et al. (2021), and b) measured surface water levels and flow discharge in AHDR.

fresh groundwater resources by the year 2100. Abd-Elaty and Polemio (2023) studied the influence of aquifer bed slopes on SWI in coastal aquifers under the impact of SLR and pumping. The study showed that when the aquifer bed sloped towards the landside, the saline intrusion was greater than when the bed slope was towards the seaside and horizontal cases.

The Nile Delta is a semi-confined aquifer, subject to groundwater exploitations and thus exposed to critical conditions (Rigw, 1998). During the last fifty years, the population of Egypt has grown by more than three-fold while water availability has remained the same (Saleh, 2009). Subsequently, the annual share of water per capita is slashed from more than 2500 m<sup>3</sup> in the year 1950 to less than 900 m<sup>3</sup> in the year 2000, and by 2050 is projected to fall to nearly 500 m<sup>3</sup> (Wagdy, 2008). Therefore, effective, integrated and sustainable management strategies must be identified and implemented at a regional scale to preserve the hydrologic cycle components. Research gaps considering human interventions' impact on river systems and their Deltas, such as large dam construction, must be filled to achieve this purpose. This is crucial to accurately assessing the amount of renewable fresh water.

Nofal et al. (2015) simulated the SWI in the NDA; the study developed an approach for the influence of aquifer heterogeneity based on newly observed data. The aquifer SWI takes place at shallow to medium layers up to 400 m, while in the deeper layers, the groundwater fluxes are moving toward the sea. Mabrouk et al. (2019) simulated the interface of fresh-saline groundwater in the NDA. The study showed the presence of groundwater salinity due to SWI in the northern parts and the over-pumping in the eastern and southwest parts of the aquifer. Abd-Elaty et al. (2021) developed mitigation solution for SWI in the Nile Delta aquifer for different wells systems using SEAWAT code; the results showed that the recharge technique reduced the intrusion by 19.5% compared with 6.20% resulting from reduction of the pumping rates and 5.90% due to applying the brackish water abstraction.

The purpose of this study is to employ the numerical model SEAWAT for simulating the water budget and salinity for the coastal aquifer of the Nile Delta under combined effect of SLR, over-pumping, and operation of the GERD project. The model runs under different scenarios of GERD filling for 17 billion cubic meters (BCM), 37.30 BCM, and 74 BCM, which causes a reduction in the river Nile hydrograph at Aswan High Dam (AHD) by 17 BCM, 20.30 BCM, and 36.70 BCM respectively. This means the storage of the AHD will decline to reach 38.50 BCM, 35.20 BCM, and 18.80 BCM, at elevations of 600 m, 621 m, and 645 m above mean sea level (AMSL), respectively, compared to the current 55.50 BCM. This is combined with increased abstraction rates by 25%, 50%, and 100% and SLR by 25 cm, respectively. The impacts of these scenarios on water resource availability were evaluated. The approach presented here can help decision-makers identify integrated and sustainable strategies for freshwater management plans in comparable river systems and their Deltas.

## 2. Egypt and the River Nile

The river Nile runs about 6500 km from the equatorial plateau in the south to the Mediterranean Sea in the North, crossing five different climatic regions (Fig. 1a). Its catchment area covers 10% of Africa's landmass and is shared by 11 riparian countries (Siam and Eltahir, 2017). The catchment area covers  $3.35 \times 10^6$  km<sup>2</sup>, corresponding to 10% of the African continent's extension (Basheer et al. (2021). Ethiopian rivers, including the Blue Nile, the Atbara, and the Sobat, contribute to 86% of the total River Nile flow (Sutcliffe, 2009).

In 2007, the average rainfall in the Nile basin was 2000 km<sup>3</sup> per year, with about 3% of the total rainfall reaching Lake Nasser (Awulachew, 2012). In 1890, the first agreement was developed between Great Britain and Germany (i.e., the Anglo-German Agreement), and the River Nile was put under control (Tvedt, 2004). In 1902, the Nile Project Commission applied ambitious development plans for dam projects on the Sudan/Uganda border, irrigation in Sudan, and summer flooding in Egypt. In 1925, a new Water Commission was defined, leading to a Water Agreement between Egypt and Sudan in 1929. Under this new agreement, 4 billion cubic meters per year (BCM yr<sup>-1</sup>) was given to Sudan, and the rest of the yearly River Nile flow plus 48 BCM yr<sup>-1</sup> for Egypt. Moreover, the agreement assured that no construction work would be done along the River Nile or on any territory, threatening Egyptian interests (Wolf and Newton, 2011). The agreement signed in 1959 set the maximum volume of water to 55.50 BCM yr<sup>-1</sup> and 18.50 BCM yr<sup>-1</sup> for Egypt and Sudan, respectively, out of 84 BCM yr<sup>-1</sup> (El-Fadel et al., 2003). In 1969, Egypt built the Aswan High Dam (AHD) to control and manage the River Nile water flow downstream and safeguard Egypt from hazards of drought and flooding (Abu-Zeid and El-Shibini, 1997; Zeid, 1989). Fig. 1b presents the measured surface water level and flow discharge in Aswan High Dam Reservoir (AHDR), the data based on Amary (2008), Ramadan et al. (2011) and Hossen et al. (2022).

The Ethiopian government planned to build hydropower plants along the River Nile to improve water and energy security (Whittington et al., 2005). Thus, in 2011, the construction of a large-scale hydropower plant known as the GERD was initiated on the Blue River Nile. The GERD (11° 16' 00" north, 35° 17' 00" East) is in Guba, approximately 750 km Northwest of Addis Ababa. The GERD creates a reservoir with a storage water capacity of 74 BCM and an installed power capacity of 6 GW; this will significantly impact the downstream Nile flow (Mulat and Moges, 2014). In 2013, an international panel report indicated that the GERD impounding and operation would decrease the surface water levels of AHDR, reduce the power generation at AHD, and increase the Nile Delta salinity (Elsayed et al., 2013). Ramadan et al. (2011) indicated that the live storage at AHDR would reach 13.30 BCM, 25.40 BCM, 37.30 BCM, and 55.50 BCM at impounding GERD by 2, 3, and 6 years at the Nile normal flow, respectively. A study by El-Nashar and Elyamany (2018) showed that by decreasing the Nile river flow from 90% to 80% the water levels in the canal's network surface decreased. Heggy et al. (2021) suggested that the maximum permissible cut for Egypt's water share should be less than 5–15%. The GERD reservoir capacity must be agreed upon between Egypt, Sudan, and Ethiopia.

### 3. Materials and method

#### 3.1. The Nile Delta

The Nile Delta aquifer (NDA) is one of the largest groundwater reservoirs; it is located between longitudes 29° 30' and 32° 30' E and latitudes 30° 00' and 31° 45' N with an area of 25,000 km<sup>2</sup> (Fig. 2a).

##### 3.1.1. Meteorological data of the Nile Delta

The Rainfall regime in Egypt is very scarce, with an annual average of 51 mm. The precipitation rates in the study area of NDA are limited and range from 250 mm year<sup>-1</sup> in the coastal regions to 200 mm year<sup>-1</sup> in the southern and middle parts. Also, the Evaporation rates are about 4 mm day<sup>-1</sup> in the Northern parts of the Nile Delta, with an average daily temperature of between 17 °C and 20 °C (Harley et al., 2006).

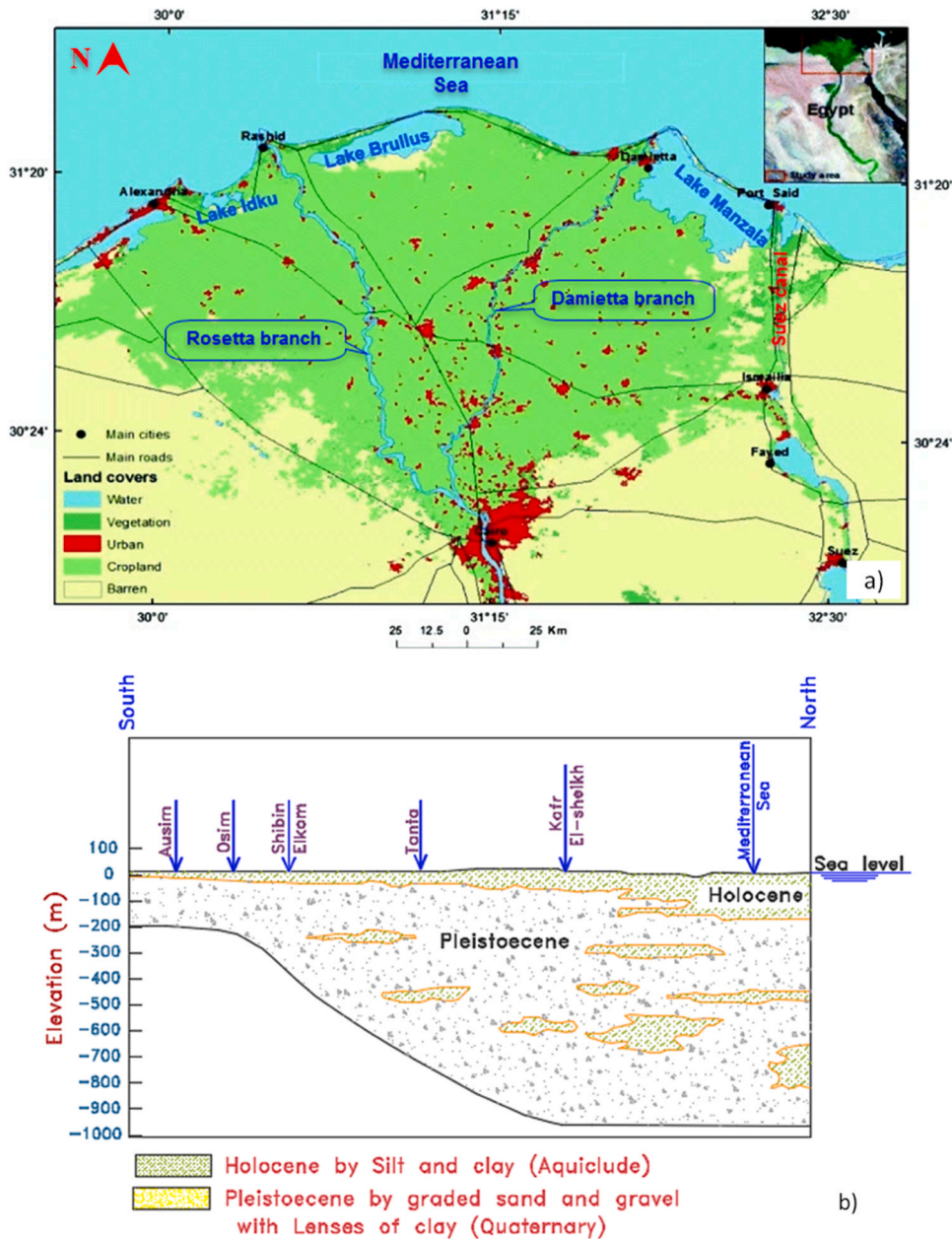


Fig. 2. An overview of the study area: a) location and horizontal extent of the Nile Delta aquifer after Hasan et al. (2015) and b) vertical hydrogeological cross-section from North to South, location of the cross-section modified after (Elewa, 2010; Abd-Elaty and Zelenakova, 2022b)

### 3.1.2. Geology of the Nile Delta

Fig. 2b presents a vertical cross-section of the NDA. The aquifer formed through the River Nile's supply of nutrients and sediment deposits. With the construction of AHD, these deposits were reduced, and the use of heavy fertilization increased. Also, the salinity of coastal lagoons increased (Rigw, 1992).

The aquifer comprises two geological deposits; the deepest Tertiary aquifers contain Eocene, Oligocene, Miocene, and Pliocene rock deposits (El Shinawi et al., 2022b). The second is the Quaternary aquifer, which includes Holocene and Pleistocene deposits with sands, clays, and gravels. The Quaternary sediments have considerable variations in their lateral and vertical lithological facies; they are composed of graded sands and gravels with clay lenses (Rigw, 1992). The thickness of the Quaternary aquifer of the Nile Delta (Mit Ghamr Formation) increases from South to North.

Quaternary deposits are represented by the Nile sediments (Sallouma, 1983). It includes the Holocene and Pleistocene sediments, and the deposits' thickness increases Northward to 250 m in the south and 1000 m in the North. The maximum thickness of Holocene deposits is about 77 m (Rigw, 1992).

### 3.1.3. Hydrogeology of the Nile Delta

The Mediterranean Sea bounds the NDA from the north for 300 km and the Suez Canal, from the east, for about 75 km. Also, Ismailia and Nubaria canals bound southeast and southwest, respectively. NDA has a length of about 200 km from the north to the south (El-Din, 2013; El Shinawi et al., 2022a). The two branches of the river Nile, including the Rosetta branch in the West and the Damietta branch in the east, draw the delta's triangle. This triangle has the baseline in the north along the coastal line and the head in the south at Cairo (Elshinawy, 2016). The ground surface varies from 18 m in the south to 5 m (AMSL) near Tanta (Saleh, 2009).

For the Quaternary aquifer, Rigw (1992) estimated the average vertical and horizontal hydraulic conductivity using laboratory experiments and pumping tests to be 2.5 mm day<sup>-1</sup>, and between 25 mm day<sup>-1</sup> and 55 mm day<sup>-1</sup>, respectively. Also, the average horizontal hydraulic conductivity was estimated to reach up to 75 m day<sup>-1</sup> and 100 m day<sup>-1</sup> by Rigw (1998), Dawoud et al. (2005), and El Shinawi et al. (2022a). Rigw (1992) also estimated the transmissivity and the storativity to be 5000 m<sup>2</sup> day<sup>-1</sup> and about 2.5 × 10<sup>-3</sup>, respectively, while Heggy et al. (2021) found that the storativity is between 10<sup>-4</sup> and 10<sup>-3</sup>. Rigw (1992) indicated that the main aquifer recharge was leakage from the irrigation canals. The excess water from the irrigation process and precipitation value are the main aquifer recharge ranges between 0.25 mm day<sup>-1</sup> and 0.80 mm day<sup>-1</sup>. Heggy et al. (2021) presented the aquifer abstraction; the study indicated that the wells extraction increased from 1980 to 2010, where it reached about 4.60 BCM year<sup>-1</sup>.

## 3.2. SEAWAT model

A combination of MODFLOW-2000 (Harbaugh et al., 2000) and MT3DMS (Zheng and Wang, 1999) were developed in a single code by SEAWAT. The third version of SEAWAT-2000 was documented by (Langevin et al., 2003). The current study used SEAWAT V4 to compute fluid density and viscosity (Langevin et al., 2008). SEAWAT V4 has two new processes, including the Variable-Density Flow (VDF) process for solving the variable-density groundwater flow equation according to the equivalent freshwater head written by Guo and Langevin (2002). Eq. 1:

$$\nabla \left[ \rho \frac{\mu_o}{\mu} * K_o \left( \nabla * h_o + \frac{\rho - \rho_f}{\rho_f} * \nabla Z \right) \right] = \rho * S_{s,0} \left( \frac{\partial h_o}{\partial t} \right) + \theta * \left( \frac{\partial \rho}{\partial C} \right) \left( \frac{\partial C}{\partial t} \right) - \rho_s * q'_s \quad (1)$$

The other process is the Integrated MT3DMS Transport (IMT), which solving the advection-dispersion equation (Zheng and Wang, 1999), Eq. 2:

$$\left( 1 + \frac{\rho_b K_d^k}{\theta} \right) \left( \frac{\partial (\theta C^k)}{\partial t} \right) = \nabla \left[ \theta \left( D_m^k + \alpha \frac{q}{\theta} \right) \cdot \nabla C^k \right] - \nabla \cdot (q C^k) - q'_s * C_s^k \quad (2)$$

Where  $\rho_0$ : fluid density [ML<sup>-3</sup>];  $\mu$ : dynamic viscosity [ML<sup>-1</sup> T<sup>-1</sup>];  $h_0$ : hydraulic head [L];  $K_0$ : the hydraulic conductivity [LT<sup>-1</sup>];  $S_{s,0}$ : specific storage [L<sup>-1</sup>];  $t$ : is time [T];  $\theta$ : porosity [-];  $C$ : salt concentration [ML<sup>-3</sup>];  $q'_s$ : is a source or sink [T<sup>-1</sup>]; of fluid with density  $\rho_s$ ;  $\rho_b$ : is the bulk density [ML<sup>-3</sup>];  $K_d^k$ : distribution coefficient of species k [L<sup>3</sup> M<sup>-1</sup>];  $C^k$ : concentration of species k [ML<sup>-3</sup>];  $D$ : hydrodynamic dispersion coefficient tensor [L<sup>2</sup>T<sup>-1</sup>];  $q$ : specific discharge [LT<sup>-1</sup>]; and  $C_s^k$ : source or sink concentration [ML<sup>-3</sup>] of species k.

## 3.3. Water zone budget

The water budget includes estimating the water stored and exchanged by the rivers and lakes. The balance of the hydrological system is achieved by the water flowing into and out of the system. The United States Geological Survey (USGS) developed the following equation for estimating the water balance for small watersheds based on the principles of conservation of mass in a closed system (Sutcliffe, 2009), Eq. 3:

Inputs = Outputs + Change in Storage.

$$P + Q_{in} = E_T + \Delta S + Q_{out} \quad (3)$$

$P$  is precipitation,  $Q_{in}$  is water flow into the hydrological system,  $E_T$  is evapotranspiration,  $\Delta S$  changes in water storage, and  $Q_{out}$  is water flow out of the hydrological system.

### 3.4. Canals and drains seepage conductance

The main canals are used in the model as input components for the hydrological water balance by the river package. These include surface water, bed levels, vertical hydraulic conductivity, and thickness. Moreover, the river bed conductance is due to the interaction between the groundwater and surface water system, which depends on the head difference and the vertical hydraulic conductivity between them (Saleh, 2009). Also, the main drain in the Nile Delta was assigned and simulated similarly to the river package using a drain stage for drain elevation and hydraulic conductance of the bed layer.

The seepage from the surface water bodies depends on the conductance of the rivers, streams, and open drains. It was represented in MODFLOW (Harbaugh, 2005; McDonald and Harbaugh, 1988) and estimated using the following equation: Eq. 4.

$$C = \frac{L * W * K}{M} \quad (4)$$

Where C: Conductance [ $L_2 T^{-1}$ ]; L: reach length of the river or drain [L]; W: bed width [L]; K: bed vertical hydraulic conductivity [ $L T^{-1}$ ]; M: bed thickness [L].

### 3.5. Hydraulic parameters and boundary conditions

Fig. 3 shows the top view and cross-sections of the NDA using SEAWAT V.4. The model consists of 239 columns and 168 rows with 11 layers for active and inactive cells; the cell dimension is  $1 \text{ km}^2$ . The average thickness of the aquifer ranges from 1000 m at the coastal line to 200 m in Cairo. The aquifer is divided into the main sub-aquifer, including the aquitard and Quaternary aquifer. The first layer represented the aquitard aquifer with clay cap, and the other ten layers represented the Quaternary aquifer; these layers were divided into equal thicknesses. The study area topography varies from zero level to 18 m (AMSL).

The infiltration flow to the NDA is assigned for the model with ranges between  $0.25 \text{ mm day}^{-1}$  and  $0.80 \text{ mm day}^{-1}$ . Also, the total abstraction was applied to be  $2.78 \text{ BCM yr}^{-1}$  (Rigw (1998)). The constant head boundary conditions and the hydrological setting were set for the flow model according to the following: *the northern boundary* was assigned using zero m (AMSL) along the shoreline. Also, *the southern boundary* was assigned 16.96 m for the river Nile level. Moreover, *the southeast boundary* was assigned using a river package by Ismailia canal, the surface water levels started from 16.17 m at the south to 7.01 m (AMSL) at the East, and *the Southwest boundary* was bounded using a river package by El Rayah El Behery and Nubaria canal as the surface water levels start from 16 m in the south to

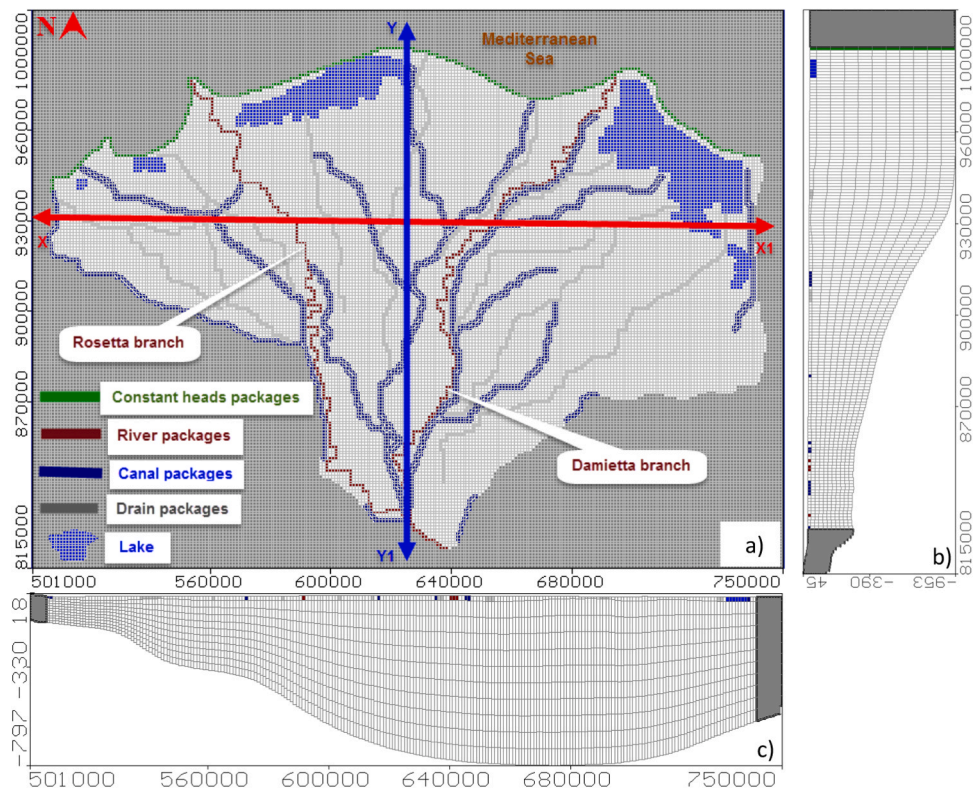


Fig. 3. Model grid and boundary conditions for the Nile Delta aquifer: a) top view, the cross-sectional view is also given according to the axis, b) X-X1 from East to West, and c) Y-Y1 from North to South.

0.5 m (AMSL) in the north.

The filling of GERD will impact the aquifer boundary conditions, in which the surface water in the irrigation canals will be lower, and the end parts will be affected by the water shortage. Also, the seepage from the irrigation network will decrease due to the lowering in the canals water surface (Tesfa, 2013). The water flow to the aquifer due to the infiltration of irrigation water will decrease and reduce net recharge. Also, over-pumping in the study area will occur due to the high water stress at the end of irrigation canals. These reasons will influence the model groundwater heads in the delta regions and the saltwater intrusion from the constant head by the Mediterranean Sea.

For the transport model, 35,000 mg L<sup>-1</sup> for the seawater TDS is assigned along the shoreline of the Mediterranean Sea. The initial groundwater concentration was set at 0 mg L<sup>-1</sup>. The input values for the aquifer hydraulic parameters are presented in Table 1.

Some previous studies collected and reported these data, and we did additional calculations. The hydraulic input parameters for the solute transport model were assigned by longitudinal, lateral, and vertical dispersivity. They were set to 100 m, 10 m, and 1 m, respectively. At the same time, the diffusion coefficient value was 10<sup>-4</sup> m<sup>2</sup> day<sup>-1</sup>.

### 3.6. Model calibration

The current calibration was developed in two stages, the first for the flow and the second for the salinity concentration. The main parameters used in calibration were aquifer hydraulic parameters, recharge, and dispersion coefficients.

The calibration was done using 81 observation wells; the minimum and maximum water head residual values (difference between the calculated and observed groundwater head values) ranged between -0.003 m and -0.973 m. The residual mean (RM) head reached -0.001 m, and the absolute RM reached 0.386 m. The RM measures the residual average, while the absolute RM measures the residual average magnitude and gives a better calibration indicator than the RM. The standard error of estimation measures the residual variability and reaches 0.052 m. The root means squared (RMS) was 0.346 m and a normalization of 3.33%, a better calibration indicator than the standard RMS (Fig. 4a).

The model calibration gave good agreement results, where the calculated head matched the field observation for the Nile Delta head map in 2008 as presented by Morsy (2009). Fig. 4b.

presents the output map of groundwater heads in the NDA. The groundwater heads range from 16 m (AMSL) to zero m from the south to the North. The study area zone budget reached 21550 m<sup>3</sup> day<sup>-1</sup>, 871700 m<sup>3</sup> day<sup>-1</sup>, 1143400 m<sup>3</sup> day<sup>-1</sup>, 9481400 m<sup>3</sup> day<sup>-1</sup>, and 11518050 m<sup>3</sup> day<sup>-1</sup> for the constant head, river leakage, canal leakage, flow into the aquifer, and total inflow, respectively.

The total outflow reached 1466800 m<sup>3</sup> day<sup>-1</sup>, 401770 m<sup>3</sup> day<sup>-1</sup>, 92632 m<sup>3</sup> day<sup>-1</sup>, 7632700 m<sup>3</sup> day<sup>-1</sup>, 1924100 m<sup>3</sup> day<sup>-1</sup>, and 11518002 m<sup>3</sup> day<sup>-1</sup> for the constant head, river leakage, canal leakage drains, and total outflow, respectively.

Moreover, Fig. 4c shows a vertical cross-section of the saltwater intrusion (SWI) distribution of TDS in the NDA. The section's thickness varies from 200 m to 1000 m, with a length of 150 km. The intrusion length reached 97.10 km for the isochlorine 35000 ppm. It encroached 70.20 km of the isochlorine 1000 ppm from the shoreline with a transition zone of 26.90 km.

### 3.7. Model scenarios

Three scenarios were tested on the Nile Delta aquifer using SEAWAT, all considering an SLR of 25 cm at the filling periods of the GERD reservoir (Table 2).

Under the first scenario (#1), a decrease of the Nile flow at Aswan High Dam (AHD) reaching 38.50 BCM was assumed due to the filling of the GERD by a water volume of 17 BCM at elevation 600 m (AMSL). In this scenario, the abstraction was increased by 25% to compensate for the reduction in the River Nile hydrograph (Fig. 5). The values are based on previous studies by Ramadan et al. (2011); Rasha and Abou Samra (2021) and AbuZeid (2021).

Under the second scenario (#2), a reduction of the Nile flow equal to 20.30 BCM corresponding to the Nile hydrograph reaching Aswan of 35.20 BCM because of the GERD filling with a water volume of 37.30 BCM at elevation 621 m (AMSL). The abstraction increased by 50% in this scenario. Under the third scenario (#3), the Nile flow equals to 18.80 BCM as a result of further water storage of 36.70 BCM in the GERD reservoir. In this third scenario, the total filling of the GERD reaches a water volume of 74 BCM at elevation 645 m (AMSL). In this scenario the abstraction in the Nile delta aquifer will reach 100% to compensate the water flow reduction in the river.

## 4. Results

The results for the water flow reaching the AHD showed a monthly variation of the basin hydrograph before the GERD operation (Fig. 6a).

**Table 1**

Input values of hydraulic properties in the Model.

Hydraulic Parameters	Horizontal hydraulic conductivity K <sub>h</sub> (m day <sup>-1</sup> )	Vertical hydraulic conductivity K <sub>v</sub> (m day <sup>-1</sup> )	Specific storage S <sub>s</sub> (m <sup>-1</sup> )	Specific yield S <sub>y</sub> (-)	Effective porosity n (%)
Aquitard	0.10–0.25	0.01–0.025	1*10 <sup>-7</sup>	0.10	50–60
Quaternary aquifer	5–100	0.50–10	0.005–0.20	0.15–0.20	30–20

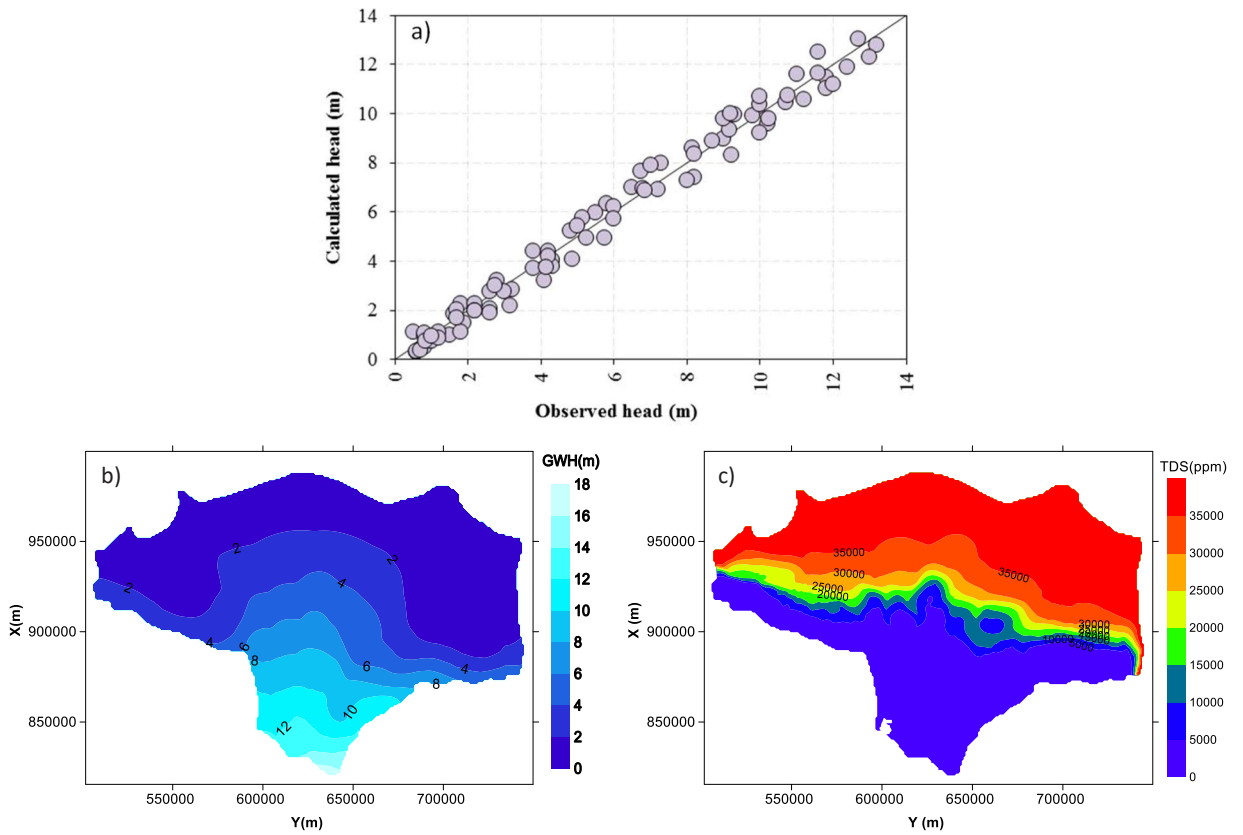


Fig. 4. Nile Delta aquifer results for: a) calculated and observed groundwater head, b) map of calculated groundwater heads, and c) map distribution of salt transport for TDS.

Table 2  
Proposed scenarios parameters.

Parameter	Baseline (2008)	scenario #1 (2022)	scenario #2	scenario #3
SLR (cm)	0	25	25	25
GERD level (AMSL)	500	600	621	645
GERD storage (BCM)	0	17	37.30	74
Reduction in Nile hydrograph (BCM) at AHD	0	17	20.30	36.70
River Nile hydrograph (BCM) at AHD	55.50	38.50	35.20	18.80
Additional abstraction (%)	0	25	75	100

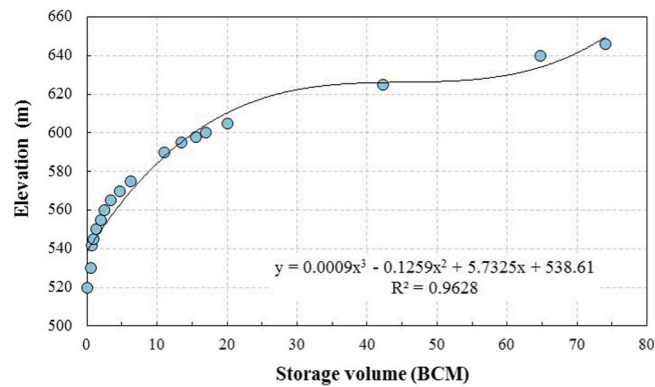


Fig. 5. The relation between the GERD storage volume and the elevation.

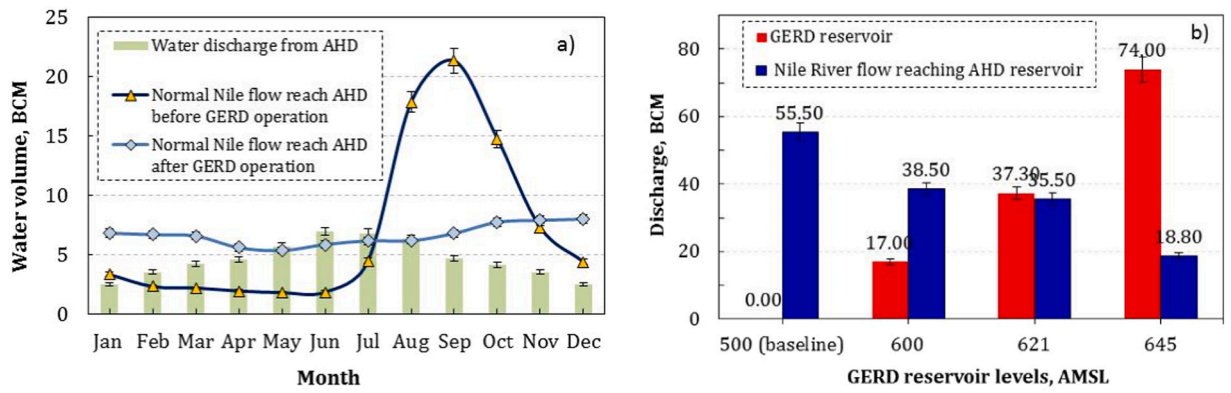


Fig. 6. Different operation scenarios of GERD: a) average monthly water demands and Nile flow reaching AHD, and b) Flow reaching AHD, and GERD reservoir filling.

A similar stable trend defined the AHD demand. However, the highest water demand is during the summer periods, thus not following the seasonal response of the basin hydrograph, which indicated the largest water volumes are during the autumn period. Overall, the results showed that the GERD reservoir filling influences the basin hydrograph, and it is required to provide yearly water volume for the operation of the AHD. More water storage must be provided during the autumn and winter to sufficiently meet demand across the summer.

Moreover, the results showed that filling of the GERD affects the normal flow hydrograph of the Nile river (55.5 BCM, the baseline case) through the operation of scenarios #1, #2, and #3, in which it will decrease the live storage of Lake Nasser to reach 38.50 BCM, 35.20 BCM, and 18.80 BCM, respectively. Those values correspond to the GERD reservoir storage levels of 600 m, 621 m, 645 m (AMSL), as presented in Fig. 6b (the lake storage is 90.7 BCM at normal conditions).

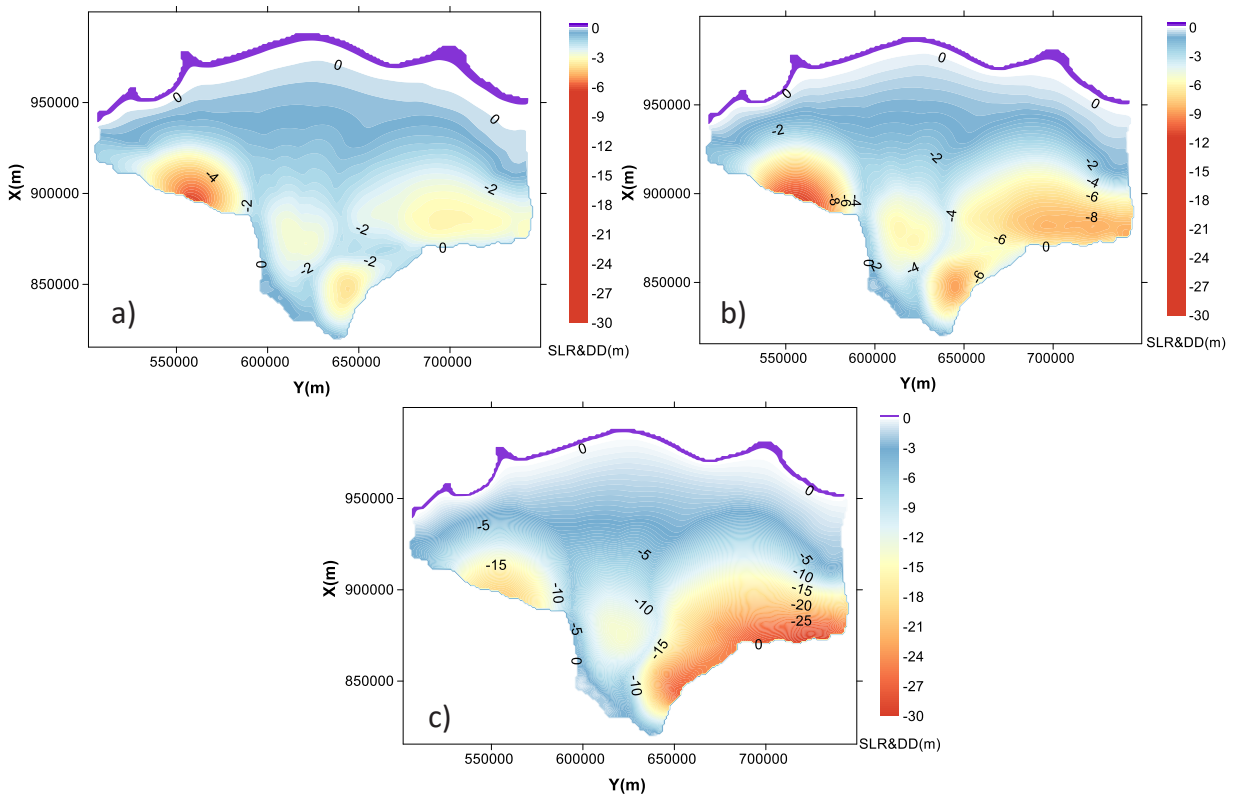


Fig. 7. Groundwater drawdown under a) the first scenario (#1), b) the second scenario (#2), and c) the third scenario (#3).

4.1. Impact of SLR, reduction in Nile hydrograph, and over-pumping on the water budget

Fig. 7 shows the impact of the three Scenarios on groundwater drawdown corresponding to the GERD reservoir storage levels of 600 m, 621 m, and 645 m (AMSL). It indicated that the groundwater drawdown at the middle part of the aquifer is greater than in the North and South due to the concentration of abstraction wells in these regions. The main sources of water supply are in the south.

The results of the head zone budget for source IN and sink OUT are presented in Fig. 8.

The results indicated that the Influx through the constant head (i.e., the Mediterranean Sea), which means the Influx through the constant head boundary reached 2086430 m<sup>3</sup> day<sup>-1</sup>, 4751450 m<sup>3</sup> day<sup>-1</sup>, and 9926000 m<sup>3</sup> day<sup>-1</sup> compared with 893250 m<sup>3</sup> day<sup>-1</sup> at the baseline case with changes of 7.76%, 18.71%, 39.19%, 64.73% for the baseline case and the scenario #1, #2, #3 respectively (Fig. 8a).

The canals leakage reached 2037300 m<sup>3</sup> day<sup>-1</sup>, 2157600 m<sup>3</sup> day<sup>-1</sup>, and 2277900 m<sup>3</sup> day<sup>-1</sup> for the three scenarios and 1143400 m<sup>3</sup> day<sup>-1</sup> (Table 3) at the baseline case with changes of 9.93%, 18.27%, 17.79%, and 14.86% for the baseline case and the scenario #1, #2, #3 respectively. The recharge into the aquifer reached 9481400 m<sup>3</sup> day<sup>-1</sup>, 7027000, 5215900 m<sup>3</sup> day<sup>-1</sup>, and 3129400 m<sup>3</sup> day<sup>-1</sup> in the baseline case and scenarios #1, #2, and #3, respectively, with changes of 82.32%, 63.02%, 43.02%, and 20.41%, respectively. The total inflow reached 11150730 m<sup>3</sup> day<sup>-1</sup>, 12124950 m<sup>3</sup> day<sup>-1</sup>, and 15333300 m<sup>3</sup> day<sup>-1</sup> for scenarios 1, 2, 3, respectively, compared with 11518050 m<sup>3</sup> day<sup>-1</sup> at the baseline case. The increase in the total inflow is due to the influence of saline water that enters the hydrological system due to the shortage of water supplies.

In total, the results of canal leakage reached 32919 m<sup>3</sup> day<sup>-1</sup>, 27863 m<sup>3</sup> day<sup>-1</sup>, and 22806 m<sup>3</sup> day<sup>-1</sup> compared with 92632 m<sup>3</sup> day<sup>-1</sup> at the baseline case, which represent changes of 0.80%, 0.30%, 0.23%, and 0.15% for the baseline case and Scenarios #1, #2, and #3 and respectively. The constant head reached 1868570 m<sup>3</sup> day<sup>-1</sup> at the baseline case and 926856 m<sup>3</sup> day<sup>-1</sup>, 482710 m<sup>3</sup> day<sup>-1</sup>, and 39490 m<sup>3</sup> day<sup>-1</sup> for the three scenarios, with changes of 16.22%, 8.31%, 3.98%, and 0.26%, respectively (Fig. 8b). The drain water budget baseline case reached 1924100 m<sup>3</sup> day<sup>-1</sup>, and 650050, 165290, and 5634 m<sup>3</sup> day<sup>-1</sup> for scenarios 1, 2, and 3 respectively. This s a changes of 16.71%, 5.83%, 1.36%, and 0.04% for the baseline case and scenarios #1, #2, #3 respectively. The well water budget reached 9540900, 11449000, and 15265000 m<sup>3</sup> day<sup>-1</sup> for the three scenarios and 7632700 m<sup>3</sup> day<sup>-1</sup> at the baseline case, which represents changes of 66.27%, 85.56%, 94.43%, and 99.56% at the baseline case and the scenario #1, #2, #3 respectively. The total outflow reached 11518002 m<sup>3</sup> day<sup>-1</sup>, 11150725 m<sup>3</sup> day<sup>-1</sup>, 12124892 m<sup>3</sup> day<sup>-1</sup>, and 15332930 m<sup>3</sup> day<sup>-1</sup> for the baseline and Scenario #1, #2, and #3, respectively (Table 3). The results show that the total outflow increased in Scenarios #1, #2, and #3 compared to the baseline case because over-pumping led to increased inflow from the constant head at Mediterranean sea at north, which increased the seawater intrusion into the aquifer.

4.2. Impact of SLR, reduction in Nile hydrograph, and over-pumping on aquifer salinity

A combined SLR by 25 cm, over-pumping by 25%, 50%, and 100% at filling of the GERD reservoir in scenarios #1, #2, and #3 (Fig. 8), reduction in Nile hydrograph was applied to the solute transport model using the SEAWAT code. The intrusion length of the isochlorine 35000 ppm advanced to 106.35 km, 110.90 km, and 114.60 km respectively for the scenarios 1,2, and 3. These intrusion lengths are measured from the shoreline. In comparison, the isochlorine 1000 ppm reached 71.15 km, 72.70 km, and 72.60 km, with transition zones of 35.20 km, 38.20 km, and 42 km (Fig. 9), which corresponds to the GERD reservoir storage levels of 600 m, 621 m, 645 m (AMSL) combined with SLR and over-pumping as shown in table 2.

The salt mass balance increased to 232000 kg, 249436 kg, and 316834 kg for the source, which represents an increase of 4.61%, 12.48%, and 42.87% relative to the baseline case, which has salt mass of 221766 kg. The salt mass for the sink out reached 133135 kg at the baseline case and increased to 139397 kg, 150600 kg, and 201465 kg, which represents an increase of 4.70%, 13.12%, and 51.32% in scenarios #1, #2, and #3, respectively, relative to the baseline case. The total in increased to 232075 kg, 249477 kg, and 316918 kg with 4.62%, 12.46%, and 42.86% compared with 221831 kg at the baseline case, while the total out increased to 232078 kg, 249481 kg, and 316835 kg with 4.62%, 12.46% and 42.82% relative to the baseline case compared with 221837 kg at the

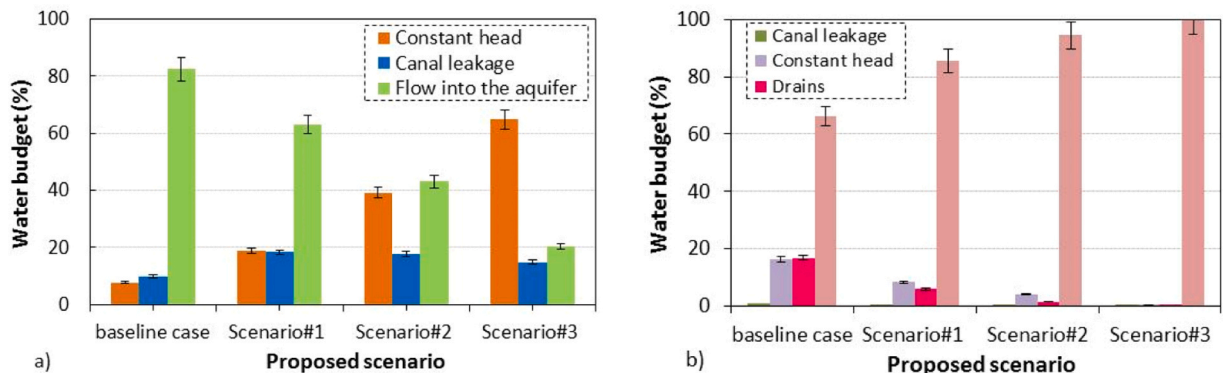
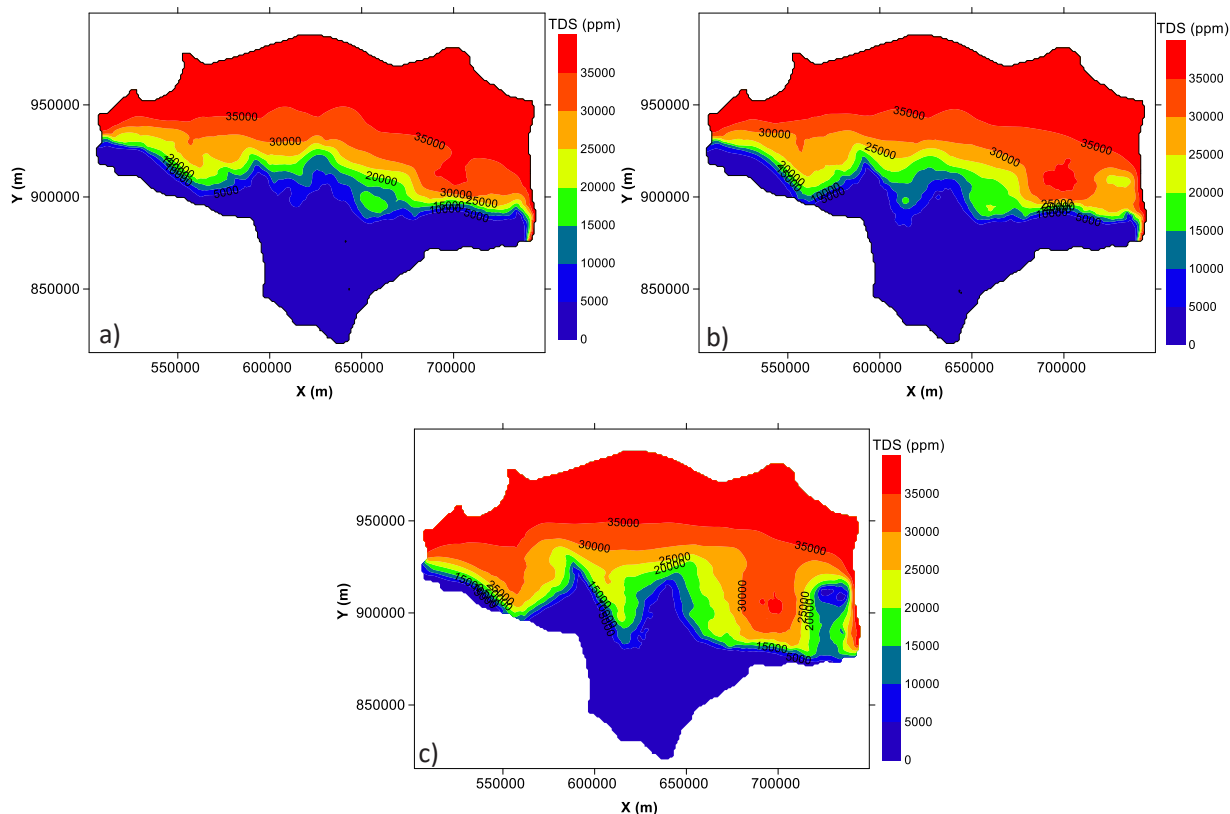


Fig. 8. Water budget analysis percentage for proposed scenarios.

**Table 3**Zone budget analysis for the proposed scenarios of GERD filling elevation (values in  $\text{m}^3 \text{day}^{-1}$ ).

Boundary parameter	Baseline Case	Scenario#1	Scenario#2	Scenario#3
Constant heads	893250	2086430	4751450	9926000
Canals leakage	1143400	2037300	2157600	2277900
Flow into the aquifer (recharge)	9481400	7027000	5215900	3129400
Total inflow	11518050	11150730	12124950	15333300
Canals leakage	92632	32919	27863	22806
Constant head	1868570	926856	482740	39490
Drains	1924100	650050	165290	5634
Wells	7632700	9540900	11449000	15265000
Total outflow	11518002	11150725	12124892	15332930

**Fig. 9.** Map distribution of total dissolved solids (TDS) for a) the first scenario (#1), b) the second scenario (#2), and c) the third scenario (#3).

baseline case (Table 4).

The isochlorine 35000 ppm moved farther away from the sea in the land direction (Fig. 9c), which means the saline intrusion wedge has increased. This is because the reduction in the surface water recharge because of the construction of the GERD dam led to the decline of the fresh groundwater storage in the NDA, combined with the over-abstraction of brackish and saline water. This will also increase the soil salinity and degradation of the Nile Delta's agricultural land in addition to declining crop production. It can also be noticed that the isochlorine 1000 ppm (Fig. 9c) moved on the landward side, which means the transition (dispersion) zone has been widened.

The aquifer salt mass is 92594 kg, 98814 kg, and 115214 kg for scenarios 1, 2, and 3 respectively. In comparison, the baseline case is 88634 kg, representing a change of 4.47%, 11.48%, and 29.99% in the three scenarios, respectively relative to the baseline case (Fig. 10).

## 5. Discussion

The results investigated the impact of increase of SLR by 25 cm combined with a reduction in Nile hydrograph by 17 billion cubic meters (BCM), 20.30 BCM, and 36.70 BCM because of the operation of the GERD by filling storage volumes of 17 BCM, 37.30 BCM, and

**Table 4**

Salt mass balance analysis for the proposed scenarios of GERD filling elevation (values in kg).

Parameter	Baseline case	Scenario#1	Scenario#2	Scenario#3
Source In	221766	232000	249436	316834
Sink Out	133135	139397	150600	201465
Total In	221831	232075	249477	316918
Total Out	221837	232078	249481	316835
Aquifer salt	88634	92594	98814	115214

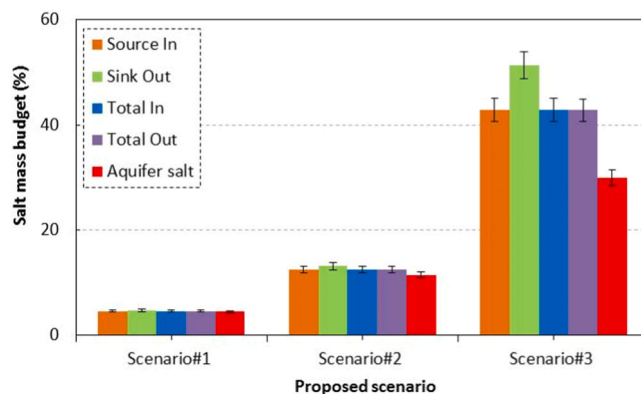


**Fig. 10.** Salt mass budget % under the different scenarios.

74 BCM respectively, on the water salinity of the Nile Delta Aquifer. Also, over-pumping by 25%, 50%, and 100% will accelerate the SWI in the Nile Delta and result in the loss of large quantities of fresh water in the aquifer. The study results showed that the freshwater recharge into the aquifer decreased by 63.02%, 43.02%, and 20.41% compared with the baseline case for the three GERD filling scenarios respectively combined with SLR and over-pumping from the aquifer (Fig. 11). These results agreed with [Mulat and Moges \(2014\)](#), which showed that the reservoir GERD would significantly impact the downstream Nile flow. This agrees with our finding for the GERD filling. Also, [Abd-Elhamid et al. \(2019\)](#) studied the GERD’s potential impacts on the Nile Delta’s water resources and soil salinity. The study showed that decreasing the surface water levels would affect groundwater heads and salinity. Furthermore, they showed that GERD would affect the Nile Delta by filling the reservoir for 2, 3, and 6 years. Moreover, [Heggy et al. \(2021\)](#) suggested that the maximum permissible cut in Egypt’s water share should be less than 5–15%. The current study found that the seawater intrusion length of the isochlorine 35000 ppm reached 106.35 km, 110.90 km, and 114.60 km, for the three scenarios, respectively. Also, the aquifer salt mass increased to 92594 kg, 98814 kg, and 115214 kg, compared with the baseline case, where the salt mass was 88634 kg. This represented an increase of 4.47%, 11.48%, and 29.99% for scenarios #1, #2, and #3, respectively, compared with the baseline case (Fig. 11).

The increase in groundwater salinity will affect the land salinity, which means irrigation with water having greater salinity and losing large quantities of fresh groundwater in the NDA by SWI. Also, the abstraction wells for irrigation and drinking water supplies will turn off due to over-pumping and SLR caused by climate change. Besides, crop productivity will be influenced by this increase in

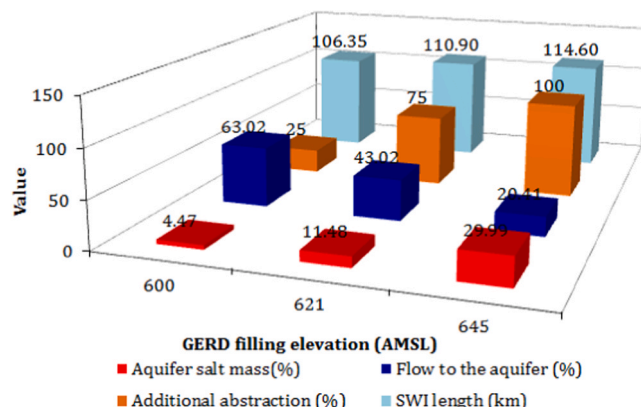


**Fig. 11.** Nile Delta aquifer under the hydrological scenario and salinity results.

salinity. It will cause a reduction in productivity and decrease food security. The study recommends that the filling and operation of the GERD dam must require integrated management between the Nile catchment basin countries to avoid the negative impact of the dam, especially at the tail of the river Nile in Egypt. This is particularly important as Egypt is the country most affected by the SLR and SWI in the North and the reduction in Nile flow in the south to avoid environmental problems and the environmental influence of New Upper Nile's Dam projects on the downstream water budget and salinity.

## 6. Conclusions

Fresh groundwater storage is a critical parameter in the hydrological system. This study numerically investigated the hydrological response of the Nile Delta aquifer (NDA) under the combined effect of SLR and the filling of the GRED dam. The filling of GERD to 17 BCM, 37.30 BCM, and 74 BCM, corresponding to GERD reservoir levels of 600 m, 621 m, and 645 m (AMSL), leads to a reduction in the River Nile hydrograph at Aswan High Dam (AHD) by 17 BCM, 20.30 BCM, and 36.70 BCM, respectively. This means the water reaching the AHD reservoir is 38.50 BCM, 35.20 BCM, and 18.80 BCM compared with 55.50 BCM in the baseline case before the GERD fillings. Moreover, the above reduction in AHD storage is combined with the abstraction rates increase in the Delta aquifer by 25%, 50%, and 100% and SLR by 25 cm for Scenario #1, 2, and 3, respectively. The total inflow reached  $11150730 \text{ m}^3 \text{ day}^{-1}$ ,  $12124950 \text{ m}^3 \text{ day}^{-1}$ , and  $15333300 \text{ m}^3 \text{ day}^{-1}$  compared with  $11518050 \text{ m}^3 \text{ day}^{-1}$  at the baseline case. This increase in the water inflow to the aquifer is mainly attributed to brackish saline water intrusion influx into the aquifer caused by wells over abstraction. In contrast, the total outflow reached  $11150725 \text{ m}^3 \text{ day}^{-1}$ ,  $12124892 \text{ m}^3 \text{ day}^{-1}$ , and  $15332930 \text{ m}^3 \text{ day}^{-1}$  compared with  $11518002 \text{ m}^3 \text{ day}^{-1}$  at the baseline case.

Our findings show that the total inflow and outflow increased in scenarios #1, #2, and #3 compared to the baseline case due to the over-pumping, which led to increased inflow from the constant head at the north, and increased seawater intrusion to the aquifer. Consequently, the GERD filling will increase the aquifer salinity and decrease the freshwater used for agriculture and domestic activities. The aquifer salt mass reached 4.47%, 11.48%, and 29.99% in GRED fillings scenarios #1, #2, and #3, respectively. This study recommends joint management between the Nile catchment countries to avoid the negative impact of this dam on water supplies in the Nile Delta for groundwater and land salinity.

### Ethics approval

Not applicable.

### Funding

This study did not receive any funding.

### CRediT authorship contribution statement

**Abd-Elaty Ismail mohammed:** Conceptualization, Data curation, Formal analysis, Funding acquisition, Investigation, Methodology, Project administration, Resources, Software, Supervision, Validation, Visualization, Writing – original draft, Writing – review & editing. **Ahmed Ashraf:** Supervision, Writing – review & editing, Funding acquisition. **Kuriqi Alban:** Methodology, Supervision, Writing – review & editing. **Ramadan Elsayed:** Data curation, Resources.

### Declaration of Competing Interest

The authors declare that they have no known competing financial interests or personal relationships that could have appeared to influence the work reported in this paper.

### Data availability

No data was used for the research described in the article.

### Acknowledgements

The authors thank the Department of Water and Water Structures Engineering, Faculty of Engineering, Zagazig University, Zagazig 44519, Egypt, for constant support during the study.

Alban Kuriqi is grateful for the Foundation for Science and Technology's support through funding UIDB/04625/2020 from the research unit CERIS.

### Code availability

Upon request.

**Authors' contributions**

Ismail Abdelaty, Alban Kuriqi, Elsayed M. Ramadan: Conceptualisation, Methodology, Investigation, Formal analysis, Data curation, Visualization, Writing–original draft, Writing–review & editing, Resources. Ismail Abdelaty, Alban Kuriqi and Ashraf Ahmed: Supervision, Writing–review & editing.

**Consent to participate**

Yes.

**Consent for publication**

Yes.

**Appendix A. Supporting information**

Supplementary data associated with this article can be found in the online version at [doi:10.1016/j.ejrh.2023.101600](https://doi.org/10.1016/j.ejrh.2023.101600).

**References**

- Abd-Elaty, I., Polemio, M., 2023. Saltwater intrusion management at different coastal aquifers bed slopes considering sea level rise and reduction in fresh groundwater storage. *Stoch. Environ. Res. Risk Assess.* <https://doi.org/10.1007/s00477-023-02381-9>.
- Abd-Elaty, I., Straface, S., Kuriqi, A., 2021. Sustainable saltwater intrusion management in coastal aquifers under climatic changes for humid and hyper-arid regions. *Ecol. Eng.* 171, 106382.
- Abd-Elaty, I., Kushwaha, N.L., Grismer, M.E., Elbeltagi, A., Kuriqi, A., 2022. Cost-effective management measures for coastal aquifers affected by saltwater intrusion and climate change. *Sci. Total Environ.* 836, 155656. DOI:<https://doi.org/10.1016/j.scitotenv.2022.155656>.
- Abd-Elaty, I., Zelenakova, M., 2022b. Saltwater intrusion management in shallow and deep coastal aquifers for high aridity regions. *J. Hydrol. Reg. Stud.* 40 <https://doi.org/10.1016/j.ejrh.2022.101026>.
- Abd-Elhamid, H., Abdelaty, I., Sherif, M., 2019. Evaluation of potential impact of Grand Ethiopian Renaissance Dam on Seawater Intrusion in the Nile Delta Aquifer. *Int. J. Environ. Sci. Technol.* 16 (5), 2321–2332. DOI:[10.1007/s13762-018-1851-3](https://doi.org/10.1007/s13762-018-1851-3).
- AbuZeid, K.M., 2021. Potential Transboundary Impacts of the Grand Ethiopian Renaissance Dam Under Climate Change and Variability. In: Diop, S., Scheren, P., Niang, A. (Eds.), *Climate Change and Water Resources in Africa*. Springer, Cham. [https://doi.org/10.1007/978-3-030-61225-2\\_16](https://doi.org/10.1007/978-3-030-61225-2_16).
- Abu-Zeid, M.A., El-Shibini, F.Z., 1997. Egypt's high Aswan dam. *Int. J. Water Resour. Dev.* 13 (2), 209–218.
- Aharmouch, A., Larabi, A., Limen, E.Md.I., 2001. Numerical modeling of saltwater interface upconing in coastal aquifers, pp. 23–25.
- Awulachew, S.B., 2012. *The Nile River Basin: water, agriculture, governance and livelihoods*. Routledge.
- Amary, W., 2008. *Study the sedimentation inside High Aswan Dam Reservoir*. M.Sc. Thesis. Faculty of engineering, Cairo University.
- Basheer, M., et al., 2021. Collaborative management of the Grand Ethiopian Renaissance Dam increases economic benefits and resilience. *Nat. Commun.* 12 (1), 5622 <https://doi.org/10.1038/s41467-021-25877-w>.
- Bear, J., 2012. *Hydraulics of groundwater*. Courier Corporation.
- Cai, W., et al., 2022. Increased ENSO sea surface temperature variability under four IPCC emission scenarios. *Nat. Clim. Change* 12 (3), 228–231. DOI:[10.1038/s41558-022-01282-z](https://doi.org/10.1038/s41558-022-01282-z).
- Canning, D.J., 2001. Climate variability, climate change, and sea-level rise in Puget Sound: Possibilities for the future.
- Dawoud, M.A., Darwish, M.M., El-Kady, M.M., 2005. GIS-baseline d groundwater management model for Western Nile Delta. *Water Resour. Manag.* 19 (5), 585–604.
- El Shinawi, A., Kuriqi, A., Zelenakova, M., Vranayova, Z., Abd-Elaty, I., 2022a. Land subsidence and environmental threats in coastal aquifers under sea level rise and over-pumping stress. *J. Hydrol.* 608, 127607.
- El Shinawi, A., Zelenáková, M., Nosair, A.M., Abd-Elaty, I., 2022b. Geo-spatial mapping and simulation of the sea level rise influence on groundwater head and upward land subsidence at the rosetta coastal zone, Nile Delta, Egypt. *J. King Saud. Univ. -Sci.*, 102145
- El-Din, M.M.N., 2013. Proposed climate change adaptation strategy for the ministry of water resources & irrigation in Egypt. *Jt. Program. Clim. Change risk Manag. Egypt*.
- Elewa, H.H., 2010. Potentialities of water resources pollution of the Nile River Delta, Egypt. *The Open Hydrology Journal* 4 (1), 1–13.
- El-Fadel, M., El-Sayegh, Y., El-Fadl, K., Khorbotly, D., 2003. The Nile River Basin: A case study in surface water conflict resolution. *J. Nat. Resour. Life Sci. Educ.* 32 (1), 107–117.
- El-Nashar, W.Y., Elyamany, A.H., 2018. Managing risks of the Grand Ethiopian renaissance dam on Egypt. *Ain Shams Eng. J.* 9 (4), 2383–2388.
- Elsayed, S.M. et al., 2013. International panel of experts (IPoE) on Grand Ethiopian Renaissance Dam project (GERDP). Addis Ababa, Ethiopia: International Panel of Experts.
- Elshinawy, H.I., 2016. Effects of Heterogeneity of Hydraulic Conductivity on Seawater intrusion in Nile Delta, Egypt MSc.
- Guo, W., Langevin, C.D., 2002. User's guide to SEAWAT; a computer program for simulation of three-dimensional variable-density ground-water flow.
- Harbaugh, A.W., Banta, E.R., Hill, M.C., McDonald, M.G., 2000. *Modflow-2000*, the U. S. Geological Survey modular ground-water model-user guide to modularization concepts and the ground-water flow process.
- Harbaugh, A.W., 2005, *MODFLOW-2005*, the U.S. Geological Survey modular ground-water model – the Ground-Water Flow Process: U.S. Geological Survey Techniques and Methods 6-A16.
- Harley, C.D.G., et al., 2006. The impacts of climate change in coastal marine systems. *Ecol. Lett.* 9 (2), 228–241.
- Hasan, E., Khan, S.I., Hong, Y., 2015. Investigation of potential sea level rise impact on the Nile Delta, Egypt using digital elevation models. *Environ. Monit. Assess.* 187 (10), 649 <https://doi.org/10.1007/s10661-015-4868-9>.
- Heggy, E., Sharkawy, Z., Abotalib, A.Z., 2021. Egypt's water budget deficit and suggested mitigation policies for the Grand Ethiopian Renaissance Dam filling scenarios. *Environ. Res. Lett.* 16 (7), 074022.
- Hossen, H., Nour-Eldeen, A.S., Negm, A., Hamdan, A.M., Elshahabi, M., Zelenakova, M., Abd-Elaty, I., 2022. Investigation of groundwater logging for possible changes in recharge boundaries and conditions in the City of Aswan. *Egypt. Water* 14, 1164. <https://doi.org/10.3390/w14071164>.
- Kumar, C.P., 2012. Climate change and its impact on groundwater resources. *Int. J. Eng. Sci.* 1 (5), 43–60.

- Langevin, C.D., Shoemaker, W.B., Guo, W., 2003. MODFLOW-2000, the US geological survey modular ground-water model—documentation of the SEAWAT-2000 version with the variable-density flow process (VDF) and the integrated MT3DMS transport process (IMT). 2331–1258.
- Langevin, C.D., Thorne Jr, D.T., Dausman, A.M., Sukop, M.C., Guo, W., 2008. SEAWAT version 4: a computer program for simulation of multi-species solute and heat transport. 2328–7055, Geological Survey (US).
- Mabrouk, M., Jonoski, A., Oude Essink, G.H.P., Uhlenbrook, S., 2019. Assessing the Fresh–Saline Groundwater Distribution in the Nile Delta Aquifer Using a 3D Variable-Density Groundwater Flow Model. *Water*. DOI:10.3390/w11091946.
- McDonald, M., Harbaugh, A.W., 1988. A Modular Three-Dimensional Finite Difference Ground-Water Flow Model. *Techniques of Water-Resources Investigations, Book 6*. U.S. Geological Survey.
- Morsy, W.S., 2009. Environmental management to groundwater resources for Nile Delta region.
- Mulat, A.G., Moges, S.A., 2014. Assessment of the impact of the Grand Ethiopian Renaissance Dam on the performance of the High Aswan Dam. *J. Water Resour. Prot.* 2014.
- Narayan, K.A., Schleeberger, C., Charlesworth, P.B., Bristow, K.L., 2002. Modeling saltwater intrusion in the lower Burdekin delta, north Queensland, Australia.
- Oude Essink, G.H.P., Schaars, F.A.M., 2003. Impact of climate change on the groundwater system of the water board of Rijnland, The Netherlands.
- Qahman, K., Larabi, A., 2006. Evaluation and numerical modeling of seawater intrusion in the Gaza aquifer (Palestine). *Hydrogeol. J.* 14 (5), 713–728.
- Ramadan, S.M., Negm, A.M., Owais, T.M., 2011. Effect of new upper Nile projects on the integrated management of the basin: Review and methodology, Fifteenth International Water Technology Conference, IWTC-15.
- Rigw, 1992. Hydrogeological Map of Nile Delta, Scale 1: 500,000. RIGW El Kanater El Khairia, Nile Delta, Egypt.
- Rigw, I., 1998. Environmental management of groundwater resources (EMGR), identification, priority setting and selection of area for monitoring groundwater quality, Technical Report TN/70.00067/WQM/97/20, Cairo, Egypt: Research Institute for ...
- Rasha M. Abou Samra, R.R. Ali, Detection of the filling phases of the Grand Ethiopian Renaissance dam using sentinel-1 SAR data, *The Egyptian Journal of Remote Sensing and Space Science*, Volume 24, Issue 3, Part 2, 2021, Pages 991-997, ISSN 1110-9823, <https://doi.org/10.1016/j.ejrs.2021.11.006>.
- Saleh, W.S.M., 2009. Environmental management of groundwater resources in the Nile Delta region.
- Sallouma, M.K.M., 1983. Hydrogeological and hydrochemical studies east of Nile Delta, Egypt.
- Sherif, M.M., Singh, V.P., 1999. Effect of climate change on sea water intrusion in coastal aquifers. *Hydrol. Process.* 13 (8), 1277–1287.
- Siam, M.S., Eltahir, E.A.B., 2017. Climate change enhances interannual variability of the Nile river flow. *Nat. Clim. Change* 7 (5), 354–350.
- Sutcliffe, J.V., 2009. The hydrology of the Nile Basin. *The Nile*. Springer., pp. 335–364.
- Tesfa, B., 2013. Benefit of grand Ethiopian renaissance dam project (GERDP) for Sudan and Egypt.
- Tiruneh, N.D., Motz, L.H., 2003. Three dimensional modeling of saltwater intrusion coupled with the impact of climate change and pumping, pp. 1–9.
- Tvedt, T., 2004. The River Nile in the age of the British: Political ecology and the quest for economic power.
- Wagdy, A., 2008. Progress in water resources management: Egypt.
- Whittington, D., Wu, X., Sadoff, C., 2005. Water resources management in the Nile basin: the economic value of cooperation. *Water Policy* 7 (3), 227–252.
- Wolf, A.T., Newton, J.T., 2011. Case Study of Transboundary Freshwater Dispute Resolution: The Nile Waters Agreement. Oregon State University, Corvallis, OR, [www.transboundarywaters.orst.edu](http://www.transboundarywaters.orst.edu) ...
- Zeid, M.A., 1989. Environmental impacts of the Aswan High Dam: a case study. *Int. J. Water Resour. Dev.* 5 (3), 14 157-157.
- Zheng, C., Wang, P.P., 1999. MT3DMS: a modular three-dimensional multispecies transport model for simulation of advection, dispersion, and chemical reactions of contaminants in groundwater systems; documentation and user's guide.